Brazilian Journal
of Chemical
Engineering

ISSN 0104-6632
Printed in Brazil
www.abeq.org.br/bjche

Vol. 36, No. 04, pp. 1727 - 1738, October - December, 2019
dx.doi.org/10.1590/0104-6632.20190364s20180583

EFFECT OF CYCLOPENTANE HYDRATES ON THE STABILITY OF DODAC AND AOT STRUCTURES

Roberta K. Rodrigues[1*], Monica F. Naccache[1] and Paulo R. S. Mendes[1]

[1] Pontifícia Universidade Católica do Rio de Janeiro, Departamento de Engenharia Mecânica, Rio de Janeiro, RJ, Brasil.
E-mail: rkamei@esp.puc-rio.br - ORCID: 0000-0003-0369-5410; E-mail: naccache@puc-rio.br - ORCID: 0000-0002-5867-5436;
E-mail: pmendes@puc-rio.br

(Submitted: December 12, 2018 ; Revised: June 26, 2019 ; Accepted: July 1, 2019)

Abstract - Hydrates are crystalline structures formed by water and substances with low molar mass molecules. Hydrate formation can occur during oil production when oil, gas and water flow through the same lines in conditions of high pressure and low temperatures. The deposition of hydrate crystals in production lines can severely jeopardize the safety of operations, being one of the biggest issues of the oil and gas industry. The present work describes a study carried out on the formation of cyclopentane hydrates. Cyclopentane forms - at atmospheric pressure - type II-structure hydrates, which are similar to those formed by natural gas. In this study, hydrate formation was induced in two different systems, one obtained with the cationic surfactant DODAC (dioctadecyldimethylammonium chloride), water, mineral oil and cyclopentane, and the other with the anionic surfactant AOT (di-(2-ethylhexyl) sulfosuccinate of sodium), water and cyclopentane. The surfactants used can form emulsions or self-associated systems, depending on compositions and concentrations of the substances that are present in the samples. The stability of the hydrates formed in the different structures was analyzed. Moreover, we also perform a study of the stability of the structures obtained when the hydrate formation is induced.
Keywords: Cyclopentane hydrate; Hydrate in emulsions; Hydrate in lamellar structures; Rheology of emulsions; Lamellar structures with hydrate.

INTRODUCTION

The transport of multiphase fluids is a critical task in deep water and cold weather conditions (Gao et al., 2008). The cost-effectiveness of fluid transportation under such conditions involves the precipitation of hydrates, asphaltenes and paraffins, and their deposition in the production lines represents one of the main problems of flow assurance. Hydrate crystals can agglomerate, forming plugs that resemble ice blocks. They can block flow lines increasing production costs, damaging equipment, reducing the efficiency of the extraction process, and compromising the safety of the operations (Vincent, 2010). For these reasons, the knowledge on hydrates has been expanded rapidly (Sloan, 2004).

Hydrates are known since at least before the beginning of the nineteenth century. In 1811, Davy (1811) detailed the composition of a hydrate as 27.7% chlorine and 72.3% water, in a molecular ratio of chlorine to water of 1:17. In 1823, Faraday and Davy (1823) synthesized chlorine hydrate in the laboratory, and proposed that water molecules form structures that act as hosts where chlorine molecules (guests) are housed. Hydrates formed by several other gases were discovered in the following years (Parrish and Prausnitz, 1972). Despite the fact that hydrates are found in nature, and that it is estimated that large volumes of natural gas are stored in this form (Sun and Englezos, 2017; Kvenvolden, 1995), the study of hydrates was only boosted in the early twentieth century, when it was detected as the cause of oil pipeline clogging (Hammerschmidt, 1934).

* Corresponding author: Roberta K. Rodrigues - E-mail: rkamei@esp.puc-rio.br

Hydrates are now described as water molecules bonded by hydrogen bonds, forming polyhedral volumes of regular hexagonal and pentagonal faces, within which low molar mass molecules are housed (Koga and Tanaka, 1996). These polyhedra are the basic building blocks of hydrates, and are found in three different structures: Type I (cubic body centered, usually formed from small molecules of natural gas), Type II (cubic face centered, usually formed by oils composed of small hydrocarbon molecules) and H-Type (hexagonal, whose cavity may contain large molecules such as naphtha) (Sloan, 1998).

Hydrate formation usually requires high pressures and low temperatures. However, cyclopentane (C5-cyclic) and tetrahydrofuran hydrates form at atmospheric pressure (Nakajima et al., 2008; Raman et al., 2016a). C5- cyclic is widely used in the study of hydrate formation, since the structure of the hydrate formed is type II, which is similar to the hydrate structure obtained with natural gas (Raman et al., 2016a; Jhaveri and Robinson, 1965). Furthermore, at atmospheric pressure, the C5-cyclic hydrate forms at temperatures as high as 7 ^{o}C (Nakajima et al., 2008). Such conditions are easily attainable in the laboratory.

An emulsion is a colloidal dispersion of two phases (immiscible liquids), where small droplets of one phase are dispersed in a continuous phase (Becher, 1965; Tadros and Vincent, 1983). Emulsions are thermodynamically unstable, but kinetic stability can be achieved with the aid of surfactants, which adsorb and form a layer at the interface between the dispersed phase and the continuous phase (Forgiarini et al., 2001). Since the interfacial energy of the system decreases with the droplet coalescence, the stability of an emulsion depends on the coalescence rate (Borwankar et al., 1992). The coalescence rate, however, depends on the height of the potential energy barrier that prevents two droplets from approaching. When this barrier is much higher than the thermal energy, the coalescing rate is almost zero and the emulsion remains stable (Borwankar et al., 1992).

In oil-in-water emulsions, the surfactant molecules are positioned so that the tail interacts with the oil droplets, and the head interacts with the water, as if they were charged oil-droplets in water. The potential energy barrier arises from the electrostatic interactions between the droplets (Shaw, 1992). The stability of the charged particles in water can be explained by the DLVO theory. According to this theory, the height of the barrier is determined by van der Waals and electrostatic forces (Hall et al., 1991; Yu and Xie, 2012). In water-in-oil emulsions, surfactants or polymer molecules adsorbed at the interface prevent droplet coalescence by a steric effect (Yu and Xie, 2012). Furthermore, the adsorbed surfactant layer decreases the tangential mobility of the droplet surfaces and decelerates the collisions between them, because it causes adsorption and interfacial tension gradients along the surfaces of two droplets as they approach – the Marangoni effect (Walstra, 1993).

Lachance et al. (2008) observed that hydrate formation and dissociation destabilize water emulsions in crude oil. It has also been observed that the hydrate formation may depend on properties of the crude oil, since it contains natural surfactants such as asphaltenes, resins and carboxylic acids, with concentrations that vary from one oil to another. Raman et al. (2016b) compared the effect on emulsion stability of the use of surfactants and emulsion-stabilizer solid particles, after hydrate formation. They concluded that water-in-oil emulsions stabilized with moderately hydrophobic solid particles resist destabilization to a greater extent than the ones stabilized with surfactants. The same was not observed in systems with highly hydrophobic particles. Kalogerakis et al. (1993) compared macroscopic characteristics of hydrate formed in a reactor containing methane gas and water with cationic, anionic or non-ionic surfactants. Hydrate formation was verified in the three systems. However, in the system with nonionic surfactat no aggregation of hydrate crystals was observed, in contrast to what happened with the cationic and anionic surfactant systems. Karaaslan and Parlaktuna (2000) also compared hydrate formation in reactors with natural gas and water with cationic, anionic and nonionic surfactants through the consumption of natural gas at different concentrations of each surfactant. In systems containing cationic and anionic surfactants, the gas consumption was higher compared to that in the absence of surfactant. However, in the system with higher concentration of cationic surfactant, the gas consumption was lower than the gas consumption in the system without surfactant. At all concentrations of non-ionic surfactant tested, gas consumption was lower than in the non-surfactant system.

In the present work, hydrates are formed from systems composed of water and oil. Experiments are carried out for a range of pH of the aqueous phase and for different temperatures, inside and outside the temperature range where hydrate formation can be observed. In this manner, the influence of these parameters on hydrate formation, and the effect of hydrates on the stability of the systems are determined and discussed. The effect of the seeding procedure, which consists of the introduction of a small amount of previously formed hydrate crystals, on the rate of hydrate formation and on the stability of the formed hydrate is also investigated. A cationic (dioctadecyldimethylammonium chloride, DODAC) and an anionic surfactant (di-(2-ethylhexyl) sulfosuccinate of sodium, AOT) are used. Depending on the compositions and concentrations of the substances in the samples, these surfactants can form emulsions or self-assembled structures.

MATERIALS AND METHODS

Two surfactants are used: Arquad 2HT-75 (dioctadecyldimethylammonium chloride, DODAC), registered trademark of Akzo Nobel Chemicals, and Aerosol OT (sodium di-(2- ethylhexyl) sulfosuccinate, AOT). Other materials used are cyclopentane (C5-cyclic) and mineral oil (Nujol, density: 0.872 g cm^{-3}, viscosity: 0.023 Pa.s, at 20 °C). Sulfuric acid (H_2SO_4) and sodium hydroxide (NaOH) were used in very low amounts, only to modify the pH of the aqueous phase of the systems. All reagents were purchased from Sigma-Aldrich and used without prior treatment.

EXPERIMENTAL PROTOCOL

Two sets of samples are studied. The formulations are prepared as described in Table 1. The stoichiometric molar ratio of water to C5-cyclic for the formation of type II hydrate is equal to 17:1. One of the samples contains excess water ("D" samples), and the other contains excess C5-cyclic ("A" samples). Sample formation is done using an ULTRA TURRAX IKA T 25 high performance disperser at 8000 rpm. During blending the samples are placed in a Thermo NESLAB RTE 17 thermal bath at 10 °C to minimize evaporation of C5-cyclic (which is highly volatile).

The samples prepared with excess water contained mineral oil to maintain the oil ratio higher than that of water, but with the stoichiometric ratio of excess water in the hydrate formation. The amount of surfactant determined for the preparation of the systems was the smallest amount in which the stability of the samples was verified. Samples with excess water remained stable for several weeks. Samples with excess C5-cyclic remained stable for approximately one week.

The rheological experiments were performed using an Anton Paar Physica MCR501 stress-controlled rheometer. This rheometer is equipped with two fixtures, a concentric cylindrical cup and a bob. The sample is positioned in the gap between the outer cylinder and the inner bob. The diameter of the inner bob is 26.6 mm and the length is 40.0 mm. The diameter of the outer cylinder is 28.92 mm and the length is 65.0 mm. Therefore, the geometry has a 2.32 mm gap. Both the outer cylinder and the inner bob are rough. They have rectangular vertical grooves, with a depth of 0.50 mm and a width of 2.60 mm, as shown in Figure 1. The dimensions of the grooves are larger than the dimensions of the structures present in the colloidal systems (1 nm - 1 μm) and larger than the emulsion droplets (which usually have a maximum size in the micrometer range). That is, the wall slip effect between the walls of the geometry and the sample is avoided with the use of the rough cylinders. In the rheometer used in the experiments, the outer cylinder is stationary, while the inner bob is part of the rotor. The outer cylinder seats into a Peltier jacket, which is mounted on the rheometer. A Thermo Haake DC 10 thermal bath with ethylene glycol solution supplies the Peltier jacket. The emulsion prepared at 10 °C is gently transferred to the outer cylinder, previously set to the same temperature. After the sample is added to the outer cylinder and the inner cylinder is fitted into the measurement position, a Teflon cap with a silica gel addition compartment is wrapped around the geometry to minimize evaporation of C5-cyclic and moisture ingress. The temperature of the samples was varied to the temperature at which the experiments were conducted at a heating/cooling rate of 0.5 °C/min. The experiments started only after the desired temperature was reached. Experiments performed with the D 7.0 system were conducted at 1.0, 4.0, 6.0, 8.0, 12.0, 15.0 and 20.0 °C. The seeding procedure was performed in some experiments by introducing into the sample, after the temperature stabilization step, a few externally prepared C5-cyclic hydrate seed crystals (approximately 0.5 g). The rheological measurements were performed by applying a constant stress of 2.0 Pa to the sample and measuring the viscosity as a function of time. Experiments with the D 8.5, D 10.0, D 12.0 and D 14.0 systems were conducted at 1.0 and 8.0 °C, without the seeding procedure. Experiments with the A 1.0, A 3.0, A 5.0 and A 7.0 systems were conducted at 1.0 °C without the seeding procedure.

The difference between the structures formed in the systems with DODAC and in the systems with AOT,

Table 1. Compositions of the systems in which hydrate formation was induced.

Solutions	Compositions (% m/m)				
	C5-cyclic	Mineral oil	DODAC	AOT	Aqueous phase
D 7.0	10.00	50.00	0.25	-	39.75 (pH 7.0)
D 8.5	10.00	50.00	0.25	-	39.75 (pH 8.5)
D 10.0	10.00	50.00	0.25	-	39.75 (pH 10.0)
D 12.0	10.00	50.00	0.25	-	39.75 (pH 11.0)
D 14.0	10.00	50.00	0.25	-	39.75 (pH 14.0)
A 1.0	79.00	-	-	1.00	20.00 (pH 1.0)
A 3.0	79.00	-	-	1.00	20.00 (pH 3.0)
A 5.0	79.00	-	-	1.00	20.00 (pH 5.0)
A 7.0	79.00	-	-	1.00	20.00 (pH 7.0)

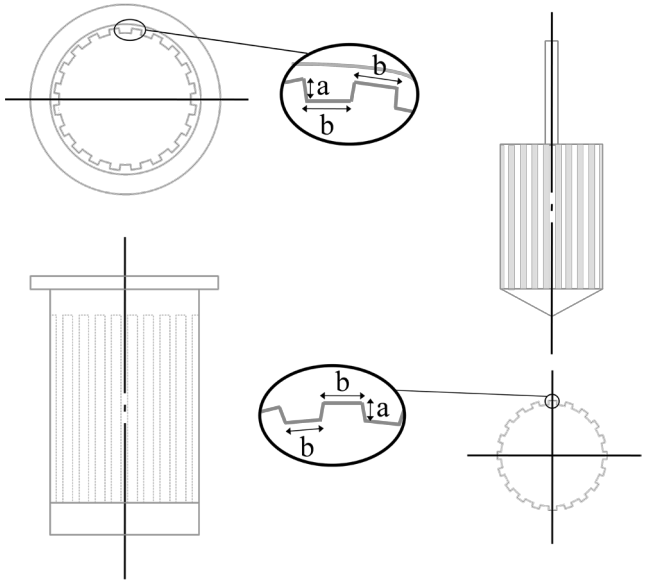

Figure 1. Scheme of the rough surface concentric cylinder rheometer geometry: the outer cylinder (left) and the inner cylinder (right). In detail, the dimensions of the grooves, where a = 0.50 mm and b = 2.60 mm.

without the presence of hydrate crystals, was obtained using X-ray diffraction (XRD) and dynamic light scattering (DLS). XRD can provide information about crystal structures and liquid crystals (Azároff, 1980). Through processed data provided by the XRD we obtain the light scattering intensity, I, as a function of the modulus q of the scattering vector q. The vector q is established from the relation between the wavelength of the incident electromagnetic radiation and the size of the object (Kittel, 2004). In this case, it represents a characteristic distance of the sample that is related to the repeat distances d between the planes of the structure, according to the equation $d = 2\pi/q$, whose constructive interference is described by Bragg's Law, as $n\lambda = 2d \sin(\theta/2)$, where n is an integer and $\theta/2$ is the Bragg diffraction angle (Kittel, 2004). The experiments were carried out using a Bruker Nanostar equipment, with an area detector Vantec 2000. The start and end angles (2θ) used were 1 and 14°, respectively. The step size was 0.02°, and the time per step was 10 seconds. The wavelength of the equipment is 1.5418 Å. The measurements were made at 20 °C.

The dynamic light scattering experiments were performed using a HORIBA SZ-100 equipment, where the scattered light intensity (at short intervals) is recorded as a function of time. Variations in the scattered light intensity are observed due to concentration fluctuations in one given volume of the solution, caused by the Brownian motion (Berne and Pecora, 2000). The time required for fluctuations to occur in scattered light intensity is the most important characteristic of the signal, since it contains information about the dynamic properties of the solute molecules (Berne and Pecora, 2000). The simplest information obtained is the translational diffusion coefficient, which for a spherical particle is related to the hydrodynamic radius R_h according to the Stokes-Einstein relation $D = k_B T/6\pi\eta_s R_h$; where k_B is the Boltzmann constant, T is the absolute temperature and η_s is the solvent viscosity (Berne and Pecora, 2000). The detector angle used was 173°. The viscosity of cyclopentane, used as solvent in the preparation of the A 1.0, A 3.0, A 5.0 and A 7.0 systems, is 4.2 x 10^{-4} Pa.s. The viscosity of the solution of mineral oil and cyclopentane 5:1 is 0.1 Pa.s. The measurements were made at 20 °C.

The experiments of viscosity as a function of time were done on five replicates (as well as the DLS and XDR experiments). Only one of these five replicates will be represented in the figures that will show the viscosity as a function of time, and light scattering intensity as a function of the scattering vector in the next section (Results and discussion). The figures that show time as a function of temperature and time as a function of pH refer to the average measures obtained from the five replicates and the error bars represent one standard deviation.

RESULTS AND DISCUSSION

The influence of the presence of hydrates on the emulsion stability is verified experimentally through viscosity measurements. Figure 2 shows the viscosity as a function of time for the system D 7.0 (see Table 1 for details), for a constant shear stress equal to 2.0 Pa

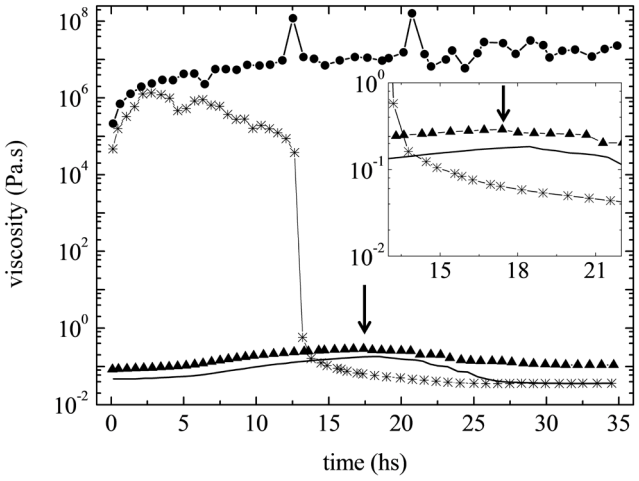

Figure 2. Viscosity as a function of time for: D 7.0 system at 1.0 °C without seeding (triangles); D 7.0 system at 1.0 °C with seeding (circles); D 7.0 system at 4.0 °C without seeding (line); and D 7.0 system at 4.0 °C with seeding (stars). Detail of the curves in the region where the destabilization of the sample is observed is shown in the insert. The arrow indicates the time when the viscosity of the system without seeding starts to decrease.

and two temperatures, namely 1.0 and 4.0 °C. These temperatures fall within the range where the C5-cyclic hydrates are formed at atmospheric pressure - $T \leq 7$ °C (Nakajima et al., 2008). The imposed shear stress or shear rate may have an influence on the hydrate formation dynamics, as discussed by Silva et al. (2017). To investigate the effect of hydrate induction, results are presented for cases with and without the seeding procedure. This procedure consists of inserting a small amount of previously formed hydrate crystals into the system whose conditions are favorable for hydrate formation. Seeding allows the growth of crystals in metastable systems, where spontaneous homogeneous nucleation may not occur or may take a long time to occur, but the growth of crystals from seeds may occur. That is, the addition of seeds to a metastable system can cause the formation of larger crystals. The seeding procedure increases the likelihood of a successful crystallization experiment. In the curves of Figure 2 referring to the experiments done without the seeding procedure it is possible to observe a slight increase in viscosity. Ahuja et al. (2018) and Chen et al. (2019) verified that the gentle viscosity increase of water-in-oil emulsions containing C5-cyclic, observed in experiments of hydrate slurry rheology is related to the precipitation of water droplets in the bottom of the outer cylinder of the geometry of the rheometer. Since the geometry of concentric cylinders has a gap between the bottom of the outer cylinder and the base of the inner bob, the precipitated water droplets may concentrate in that space. And the portion of the sheared sample between the walls of the cylinders would have a higher concentration of mineral oil, which could justify the higher viscosity. This gentle increase in viscosity may also be related to the formation of hydrate crystals. Sample aliquots were taken every hour from the beginning of the experiments and placed under a microscope. The presence of hydrate crystals was observed after three hours from the beginning of the experiment (see Figure 3a). On the other hand, Figure 2 illustrates that the seeding procedure induced the rapid formation of hydrate, leading to an abrupt increase of the viscosity. Ahuja et al. (2018) and Karanjkar et al. (2016) observed that the formation of hydrate in water-in-oil emulsions could result in the formation of a plug in the geometry of the rheometer, which caused the stress to rise above the equipment limit and, consequently, the interruption of the experiment by determination of the equipment software. These experiments were done keeping the shear rate constant. However, once the experiments shown in Figure 2 were done maintaining the stress constant, the increase of the viscosity caused by the formation of the plug in the geometry of the rheometer was compensated by the reduction of the shear rate, which avoided the interruption of the experiment by determination of the equipment software. Figure 3b shows the hydrate plug formed in the geometry of concentric cylinders.

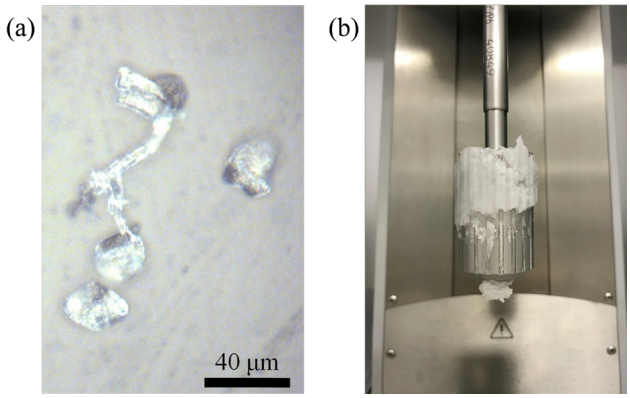

Figure 3. (a) Hydrate crystals observed in an aliquot of the D 7.0 system at 50× magnification. (b) C5-cyclic hydrate deposited on the rough surface of the upper bob of the geometry of concentric cylinders.

For the systems without seeding, it is possible to observe in Figure 2 a viscosity decrease after approximately 17 h in the experiment conducted at 1.0 °C, and after approximately 19 h in the experiment conducted at 4.0 °C. This viscosity decrease is attributed to the destabilization of the hydrate, which seems to be accelerated by the coalescence of the droplets of the emulsion induced by the approximation between them due to the agglomeration of the crystals, since the hydrate formation in emulsions occurs on the surface of the droplets (Karanjkar et al., 2012; Sakemoto et al., 2010). After 35 hours of tests, both systems showed visible phase separation.

Lachance et al. (2008) proposed a destabilization model of crude oil emulsions due to the presence of hydrates. This model is divided into two steps: formation and dissociation. The formation step can occur by two routes. If the interface around the water droplets is weak, the droplets may get too close together, leading to agglomeration. If the interface around the water droplets is strong, as it occurs for example in emulsions with high asphaltene content, they remain segregated. However, after hydrate dissociation, the guest molecules leave the aqueous medium and thus break the interface, causing coalescence of adjacent droplets.

In Figure 2 it can also be seen that the hydrate crystals formed with the seeding procedure at 1.0 °C remained stable over the 35 hours of test, when the experiment was interrupted. However, in the experiment conducted at 4.0 °C with the seeding procedure, the viscosity remained stable only until approximately 13 hours. At this point, the system destabilizes and the viscosity drops to values lower than those presented in the test carried out without the seeding procedure. This difference in behavior is

probably due to the stronger hydrate agglomeration at the lower temperature.

Previous studies (Lingelem et al., 1994; and Parent and Bishnoi, 1995) have shown that the induction-time of hydrate formation is stochastic, that is, as long as the system is maintained under metastable thermodynamic conditions, it is not possible to predict the hydrate nucleation. However, the results shown in Figure 2 illustrate that the hydrate formation process was much slower in both experiments carried out without the seeding procedure, as indicated by the fact that the viscosity level remains orders of magnitude lower than the one observed in experiments with the seeding procedure. Moreover, it seems that the presence of hydrate crystals destabilizes the emulsion before the crystals grow or agglomerate. In other words, in these emulsions there is a competition between two processes, the formation of hydrate and the coalescence of the droplets, which hinders the formation of the hydrate, since it reduces the contact area between water and C5-cyclic. When the seeding process is not carried out, the coalescence of the droplets predominates and causes the viscosity reduction.

Similar experiments (Figure 4) were also performed at 6.0, 8.0, 12.0, 15.0 and 20.0 °C without the seeding procedure, for the same shear stress of 2.0 Pa. The times at which the viscosity begins to decrease are plotted in Figure 4. In the temperature range between 8 and 20 °C, the time at which the viscosity begins to decay decreases with increasing temperature, which is in accordance with the literature (Schick and Hubbard, 2006). However, for temperatures within the range where C5-cyclic hydrates can be formed - $T \leq 7$ °C (Nakajima et al., 2008), the stability of the system increases with increasing temperature. Leopércio et al. (2016) verified in strain sweep experiments that, within a temperature range of 1.0 to 7.0 °C, the hydrate film formed at the interface between water and C5-cyclic is more structured the higher the temperature. That is, the increase in stability of the D 7.0 system with increasing temperature within the hydrate zone may be related to the formation of stronger hydrate films on the surfaces of the emulsion droplets.

The increase in viscosity with time, which can be observed with a lower intensity at 8.0, 12.0 and 15.0 °C (Figure 4a), may be related to the volatilization of C5-cyclic; however, it may also be related to packaging of water droplets in the system caused by the shear stress (Larson, 1999).

The stability of Systems D 7.0, D 8.5, D 10.0, D 12.0 and D 14.0 can be analyzed with the aid of Figure 5a, which shows the times at which a viscosity decrease is observed (for an applied constant stress equal to 2.0 Pa). The experiments were done at 1.0 and 8.0 °C. It can be noted that at both temperatures

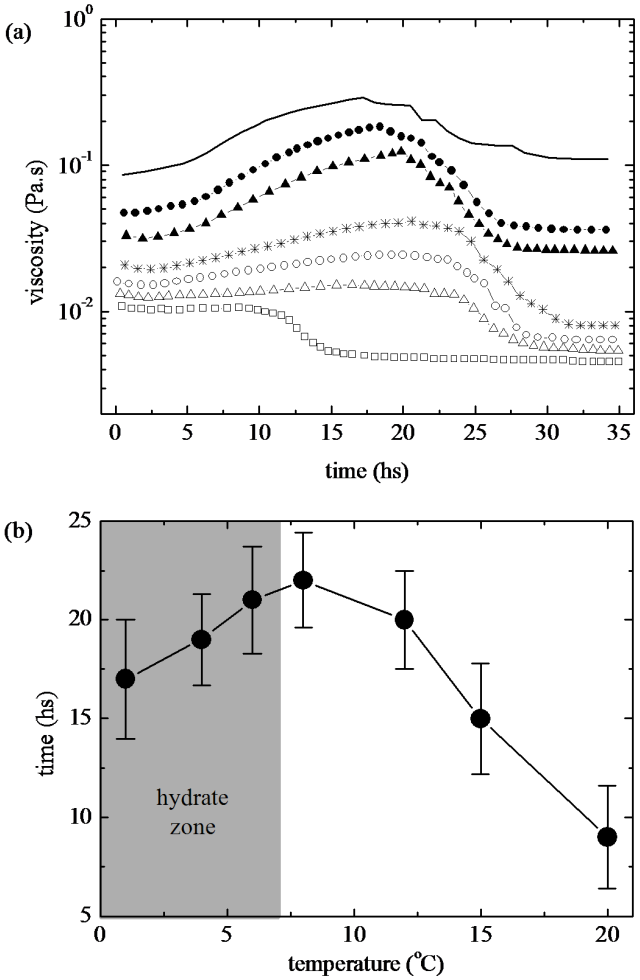

Figure 4. (a) Viscosity as a function of time for: D 7.0 system at 1.0 °C (line); D 7.0 system at 4.0 °C (full circles); D 7.0 system at 6.0 °C (full triangles); D 7.0 system at 8.0 °C (stars); D 7.0 system at 12.0 °C (empty circles); D 7.0 system at 15.0 °C (empty triangles); and D 7.0 system at 20.0 °C (empty squares). (b) Time when the viscosity of System D 7.0 without seeding starts decreasing as a function of temperature. The experiments were done with replicates. Error bars represents one standard deviation. The gray region represents the temperature range at which the hydrate formation was observed. The lines are just guides for the eyes.

the systems D 8.5, D 10.0 and D 12.0 are more stable than the systems D 7.0 and D 14.0. Figure 5b shows that the diameters of the structures formed in systems D 8.5, D 10.0 and D 12.0 are smaller than the diameters of the structures formed in systems D 7.0 and D 14.0. Since the same procedure was used to prepare all the samples, it can be concluded that the higher stability of the systems D 8.0, D 10.0 and D 12.0 is related to the smaller structures observed in these systems, which is in agreement with Abismail et al. (1999) XRD experiments have shown that these systems do not have self-organized structures, that

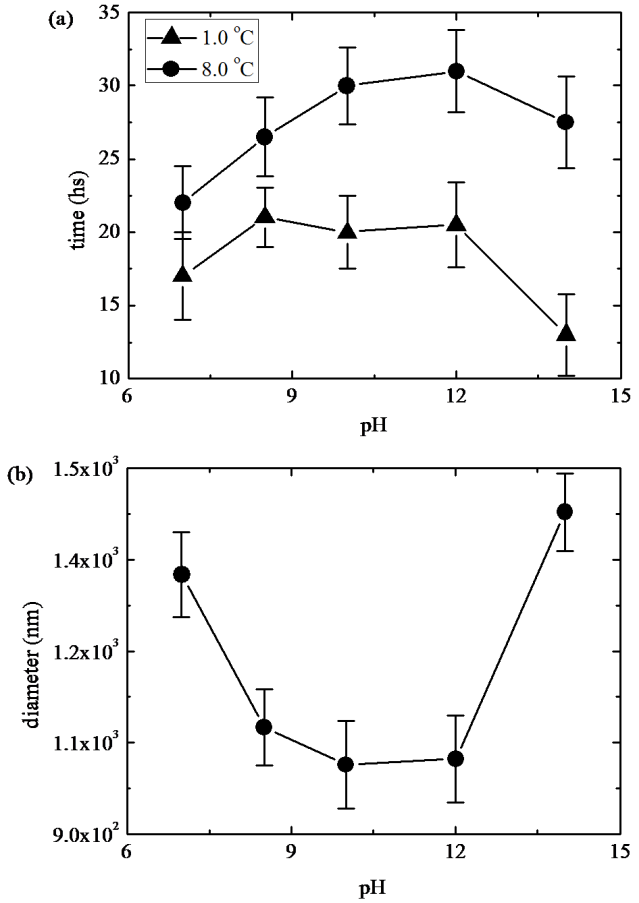

Figure 5. (a) Time when the viscosities of the systems D 7.0, D 8.5, D 10.0, D 12.0 and D 14.0 start decreasing, at temperatures of 1.0 and 8.0 °C. (b) Measurements of the diameter of the structures obtained by DLS at room temperature (20 °C). The experiments were done with replicates. Error bars represents one standard deviation. The lines are just guides for the eyes.

is, the presence of peaks was not observed in the curves of light scattering intensity as a function of the scattering vector (Figure 6). So, the systems formed are emulsions, with the structure similar to the one shown schematically in Figure 7.

Menezes et al. (2018) has verified that the formation of methane hydrate by crystallization is limited by the interface area between the water and the gas. This interfacial area may change according to the size and disposition of the water droplets.

Figure 8 shows the viscosity at 1.0 °C and τ = 2.0 Pa, for systems containing excess C5-cyclic with and without seeding. When seeding is applied, the viscosity increases at early times to quite high values, indicating the fast formation of large quantities of hydrate. When there is no seeding, it is possible to observe, under the microscope, that hydrate crystals begin to form after three hours of experiment, as in the experiments with the emulsions with excess water. After approximately 23 hours from the beginning of the experiment, an

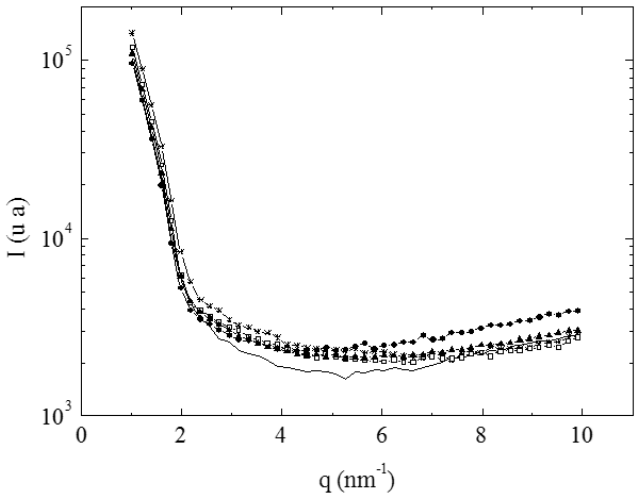

Figure 6. Light scattering intensity as a function of the scattering vector measured for systems (line) D 7.0, (full circles) D 8.5, (full triangles) D 10.0, (stars) D 12.0 and (empty squares) D 14.0, at room temperature (20 °C).

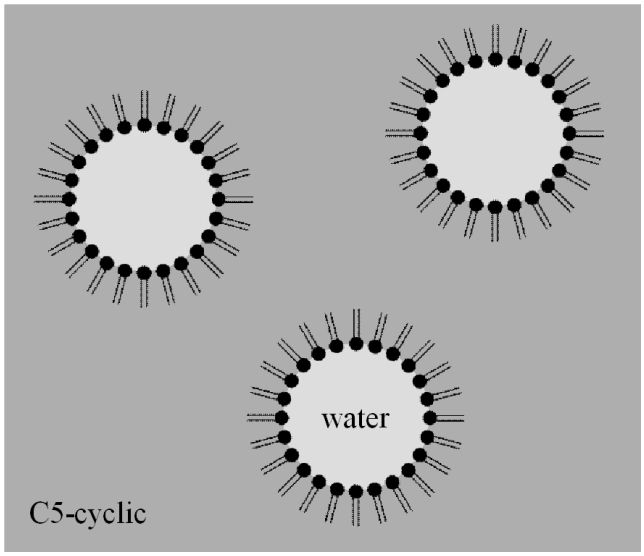

Figure 7. Representative scheme of an emulsion of water in C5-cyclic and mineral oil, prepared with the DODAC surfactant.

abrupt increase in viscosity is observed, due to the formation of larger amounts of hydrate and/or crystal agglomeration. Further on, both systems remain stable until the end of experiment at *t* 46 h.

The same viscosity experiments have been performed for the systems A 1.0, A 3.0 and A 5.0, and it was observed that these systems, as well as System A 7.0, present an increase in viscosity due to hydrate formation. Figure 9 shows the time when the viscosity of these systems increases as a function of the pH. It is seen that hydrate formation occurs earlier in samples with higher pH values (A 5.0 and A 7.0). The results shown in Figure 8 showed that the hydrate formation time of these structures is also not stochastic. The

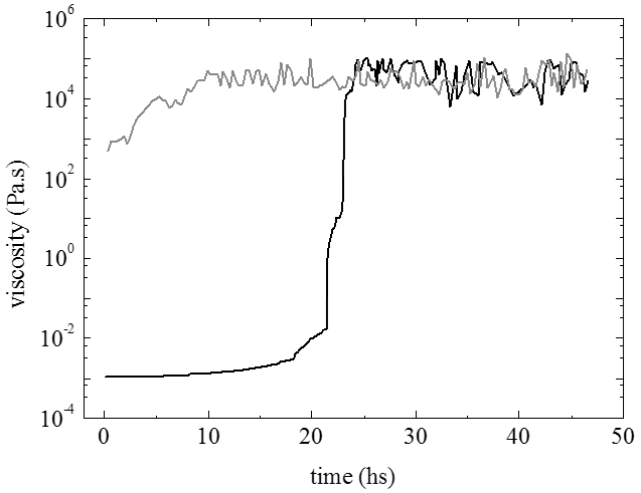

Figure 8. Viscosity as a function of time for system A 7.0. The black line represents the data obtained without seeding, and the gray line represents the data obtained with seeding.

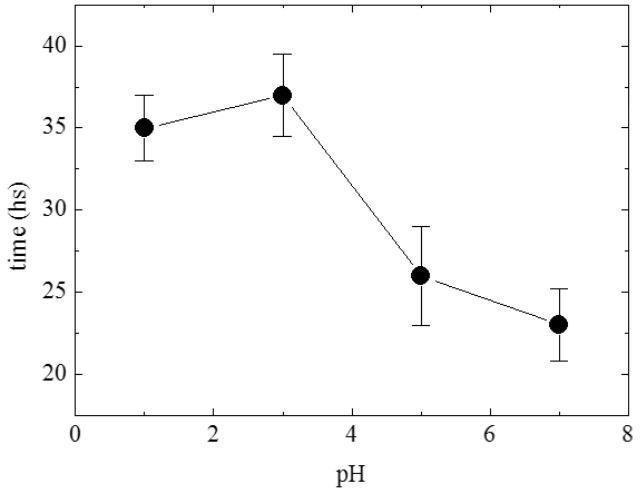

Figure 9. Time at the point of viscosity increase for A 1.0, A 3.0, A 5.0 and A 7.0, for temperature equal to 1.0 °C. The experiments were done with replicates. Error bars represents one standard deviation. The lines are guides for the eyes.

different pH values of the aqueous phase may affect the stability of the systems and the amount of water in the droplets of the emulsions or layers of the self-associated systems, which may cause the nucleation of the hydrate crystals not to be stochastic.

It is known that AOT surfactant can form lamellar structures (Boissière et al., 2002), i.e., alternating layers of water and oil separated by layers of surfactant. Therefore, the characterization of the systems containing AOT was done through XRD and DLS experiments. Figure 10 shows the light scattering intensity I as a function of the modulus of the scattering vector q, obtained by XRD experiments.

The curves for the systems A 1.0, A 3.0 and A 5.0 present two bands. The presence of peaks (or bands)

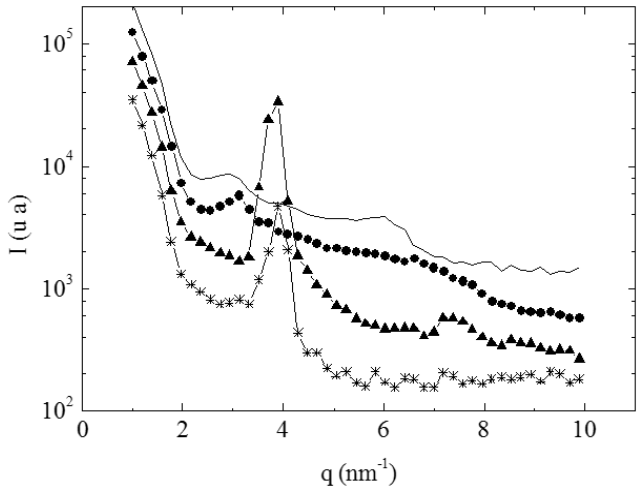

Figure 10. Light scattering intensity as a function of the scattering vector measured for systems (line) A 1.0, (circles) A 3.0, (triangles) A 5.0 e (stars) A 7.0, at room temperature (20 °C).

in XRD curves is an indication of the presence of organized systems. The higher and narrower a band, the more organized is the system. When the second peak occurs at a scattering vector modulus equal to twice the one of the first peak, it is likely that the present organized system is lamellar (Bernardes et al., 2006; Bernardes et al., 2011). Moreover, the distance d between the surfactant layers oriented in the same direction can be obtained through the relation $D = 2\pi/q$; where q_{max} is the value of modulus of the scattering vector of the first peak (Bernardes et al., 2006; Bernardes et al., 2011). The curve for the system A 1.0 presents two bands, the first one at $q^1_{max} = 2.9$ nm^{-1}, and the second one at $q^2_{max} = 5.8$ nm^{-1}. Then, the formed structure should be lamellar, and the distance between the surfactant layers oriented in the same direction in this system is $d_{A\,1.0} = 2.2$ nm. The curve referring to the system A 3.0 presents two bands: $q^1_{max} = 3.3$ nm^{-1} and $q^2_{max} = 6.6$ nm^{-1}. So, the formed structure is likely to be lamellar, and the distance between the surfactant layers oriented in the same direction in this system is $d_{A\,3.0} = 2.0$ nm. The curve for the system A 5.0 also presents two bands, with $q^1_{max} = 3.8$ nm^{-1} and $q^2_{max} = 7.6$ nm^{-1}. Again, the formed structure should be lamellar and the distance between the surfactant layers oriented in the same direction in this system is $d_{A\,5.0} = 1.6$ nm.

The system A 7.0 presented only one narrow band at approximately 4 nm^{-1}. This may indicate that this system has a high organization; however, the distance between the layers may not be homogeneous throughout the sample. The size of a molecule of the surfactant AOT is estimated to be between 7 and 15 Å (Eskici and Axelsen, 2016). Therefore, the distance obtained between the layers of surfactant is consistent, since the tails of the surfactants, positioned in opposite directions covering a C5-cyclic layer, can intertwine.

Unlike the emulsions, the lamellar structures are thermodynamically stable, which may explain why the systems A 1.0, A 3.0, A 5.0 and A 7.0 remain stable, while the systems D 7.0, D 8.5, D 10.0, D 12.0 and D 14.0 destabilize.

Figure 11 shows the diameter of the structures of the aqueous solution used in the preparation of the systems, as a function of the pH. The measurements were obtained using DLS, and applying the Stokes-Einstein relation for the translational di□usion. From largest to smallest, the order of diameters measured for the systems was: A 3.0, A 1.0, A 5.0 and A 7.0, which is the same sequence observed for the time of the beginning of viscosity increase due to the hydrate formation. Since the amount of the aqueous solution, C5-cyclic and AOT are the same in all samples, then systems with smaller structures seem to contain more structures and therefore the interfacial area is larger, leading to more nucleation sites for hydrate formation. The results shown in Figure 9 showed that the pH of the aqueous phase of the systems can affect the hydrate formation time, since it affects the organization of the structures.

The structures formed in the systems A 1.0, A 3.0, A 5.0 and A 7.0 are shown schematically in Figure 12. According to the results obtained in the XDR experiments, the distance between the surfactant layers oriented in the same direction in the A 1.0 system is 2.2 nm. And according to the results obtained in the DLS experiments, the diameter of the structures present in the A 1.0 system is approximately 640 nm. Figure 12a shows a representative scheme of the structures present in the A 1.0 system. The distance between the surfactant layers oriented in the same direction in the A 3.0 system is 2.0 nm. And the diameter of the structures present in the A 3.0 system is approximately 680 nm. Figure 12b shows a representative scheme of the structures present in the A 3.0 system. The distance between the surfactant layers oriented in the same direction in the A 5.0 system is 1.6 nm. And the diameter of the structures present in the A 5.0 system is approximately 550 nm. Figure 12c shows a representative scheme of the structures present in the A 5.0 system. The XDR experiments showed that the distance between the surfactant layers oriented in the same direction in the A 7.0 system is indefinite. This may indicate that this system has a high organization, however, the distance between the layers may not be homogeneous throughout the sample. And the diameter of the structures present in system A 7.0 is approximately 285 nm. Figure 12d shows a representative scheme of the structures present in system A 7.0. That is, comparing the systems A 1.0, A 3.0, A 5.0 and A 7.0, the distance d between the surfactant layers oriented in the same direction decreases in the following sequence: $d_{A\ 1.0} > d_{A\ 3.0} > d_{A\ 5.0}$. The distance $d_{A\ 7.0}$ could not be determined. The diameter of the structures decreases in the following sequence: $L_{A\ 3.0} > L_{A\ 1.0} > L_{A\ 5.0} > L_{A\ 7.0}$.

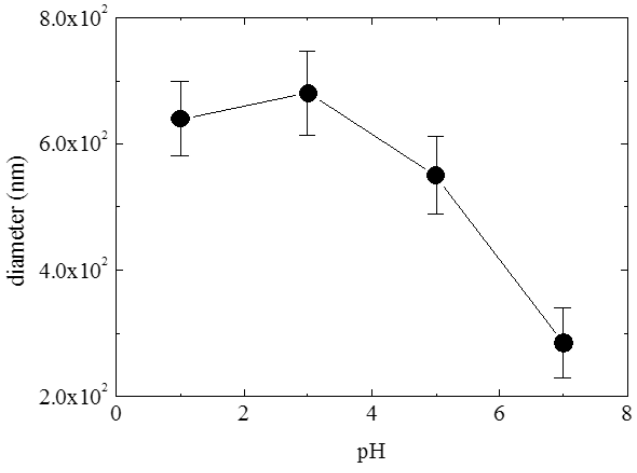

Figure 11. Diameter of the structures formed in Systems A 1.0, A 3.0, A 5.0 and A 7.0, obtained with DLS, at room temperature (20 °C). The experiments were done with replicates. Error bars represent one standard deviation. The lines are just guides for the eyes.

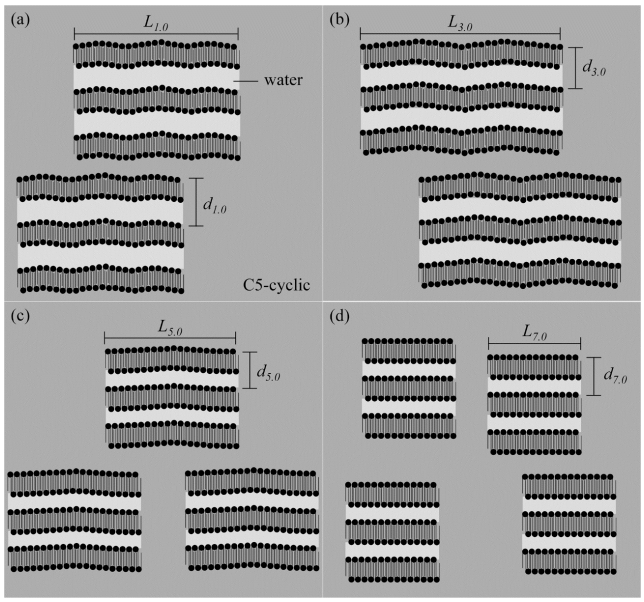

Figure 12. Representative scheme of lamellar structures formed by C5-cyclic, AOT and (a) aqueous solution with pH 1.0, (b) aqueous solution with pH 3.0, (c) aqueous solution with pH 5.0, and (d) aqueous solution with pH 7.0. XDR experiments indicated that $d_{A\ 1.0} > d_{A\ 3.0} > d_{A\ 5.0}$. The distance $d_{A\ 7.0}$ could not be determined. DLS experiments indicated that $L_{A\ 3.0} > L_{A\ 1.0} > L_{A\ 5.0} > L_{A\ 7.0}$.

FINAL REMARKS

A study was carried out about the behavior of systems containing C5-cyclic, water and two different

surfactants, submitted to favorable conditions for hydrate formation. The effect of temperature, pH, and hydrates on the stability of the systems was evaluated through rheological measurements. The results indicate that the presence of hydrate crystals reduce the emulsion stability. The results also indicate that the pH affects the diameter of the structure and, consequently, the stability of the systems. It was also observed that intermediate pH values lead to more stable systems, because their structure diameters are smaller. It was also shown that hydrates form earlier as the pH increases. Light scattering measurements were also performed and revealed that systems with excess C5-cyclic tend to form more organized lamellar structures, which are thermodynamically stable, in contrast to the emulsions, which are the structures formed in the systems with excess water. This should explain why systems with excess C5-cyclic remain stable for longer times, even in the presence of hydrates.

ACKNOWLEDGEMENT

The authors thank Petrobras S.A., CNPq, CAPES, FAPERJ, and FINEP for the financial support.

REFERENCES

Abismail, B., Canselier, J. P., Wilhelm, A. M., Delmas, H., Gourdon, C. Emulsification by ultrasound: drop size distribution and stability. Ultrasonics Sonochemistry, 6, 75-83 (1999). https://doi.org/10.1016/S1350-4177(98)00027-3

Ahuja, A., Iqbal, A., Iqbal, M., Lee, J. W., Morris, J. F. Rheology of hydrate-forming emulsions stabilized by surfactant and hydrophobic silica nanoparticles. Energy & Fuels, 32, 5877-5884 (2018). https://doi.org/10.1021/acs.energyfuels.8b00795

Azároff, L. V. X-Ray Diffraction by Liquid Crystals. Molecular Crystals and Liquid Crystals, 60, 73-98 (1980). https://doi.org/10.1080/00268948008072426

Becher, P. Emulsions: Theory and Practice, Reinhold, New York (1965).

Bernardes, J. S., Norrman, J., Piculell, L., Loh, W. Complex Polyion-Surfactant Ion Salts in Equilibrium with Water: Changing Aggregate Shape and Size by Adding Oil. Journal of Physical Chemistry B, 110, 23433-23442 (2006). https://doi.org/10.1021/jp0636165

Bernardes, J. S., Piculell, L., Loh, W. Self-Assembly of Polyion-Surfactant Ion Complex Salts in Mixtures with Water and *n*-Alcohols. Journal of Physical Chemistry B, 115, 9050-9058 (2011). https://doi.org/10.1021/jp202413q

Berne, B. J., Pecora, R. Dynamic Light Scattering: With Applications to Chemistry, Biology, and Physics, John Wiley & Sons, New York (2000).

Boissière, C., Brubach, J. B., Mermet, A., Marzi, G. de, Bourgaux, C., Prouzet, E., Roy, P. Water Confined in Lamellar Structures of AOT Surfactants: An Infrared Investigation. The Journal of Physical Chemistry B, 106, 1032-1035 (2002). https://doi.org/10.1021/jp012724i

Borwankar, R. P., Lobo, L. A., Wasan, D. T. Emulsion stability - kinetics of flocculation and coalescence. Colloids and Surfaces, 69, 135-146 (1992). https://doi.org/10.1016/0166-6622(92)80224-P

Chen, Y., Shi, B., Liu, Y., Ma, Q., Song, S., Ding, L., Lv, X., Wu, H., Wang, W., Yao, H., Gong, J. In-Situ Viscosity Measurements of Cyclopentane Hydrate Slurry in Waxy Water-in-Oil Emulsions. Energy & Fuels, 33, 2915-2925 (2019). https://doi.org/10.1021/acs.energyfuels.8b04268

Davy, H. On a combination of oxymuriatic gas and oxygene gas. Philosophical Transactions of the Royal Society of London, 101, 155-162 (1811). https://doi.org/10.1098/rstl.1811.0008

Eskici, G., Axelsen, P. H. The Size of AOT Reverse Micelles. The Journal of Physical Chemistry B, 120, 11337-11347 (2016). https://doi.org/10.1021/acs.jpcb.6b06420

Faraday, M., Davy, H. On Fluid Chlorine. Philosophical Transactions of the Royal Society of London, 113, 160-165 (1823). https://doi.org/10.1098/rstl.1823.0016

Forgiarini, A., Esquena, J., Gonzáles, C., Solans, C. Formation of Nano-emulsions by Low-Energy Emulsification Methods at Constant Temperature. Langmuir, 17, 2076-2083 (2001). https://doi.org/10.1021/la001362n

Gao, S. Investigation of Interactions between Gas Hydrates and Several Other Flow Assurance Elements. Energy & Fuels, 22, 3150-3153 (2008). https://doi.org/10.1021/ef800189k

Hall, S. B., Duffeld, J. R., Williams, D. R. A reassessment of the applicability of the DLVO theory as an explanation for the Schulze-Hardy rule for colloid aggregation. Journal of Colloid and Interface Science, 143, 411-415 (1991). https://doi.org/10.1016/0021-9797(91)90274-C

Hammerschmidt, E. G. Formation of Gas Hydrates in Natural Gas Transmission Lines. Industrial and Engineering Chemistry, 26, 851-855 (1934). https://doi.org/10.1021/ie50296a010

Jhaveri, J., Robinson D. B. Hydrates in the Methane-Nitrogen System. The Canadian Journal of Chemical Engineering, 43, 75-78 (1965). https://doi.org/10.1002/cjce.5450430207

Kalogerakis, N., Jamaluddin, A. K. M., Dholabhai, P. D., Bishnoi, P. R. Effect of Surfactants on Hydrate Formation Kinetics. SPE International Symposium on Oilfield Chemistry. Louisiana (1993). https://doi.org/10.2118/25188-MS

Karaaslan, U., Parlaktuna, M. Surfactants as Hydrate Promoters? Energy & Fuels, 14, 1103-1107 (2000). https://doi.org/10.1021/ef000069s

Karanjkar, P. U., Lee, J. W., Morris, J. F. Calorimetric investigation of cyclopentane hydrate formation in an emulsion. Chemical Engineering Science, 68, 481-491 (2012). https://doi.org/10.1016/j.ces.2011.10.014

Karanjkar, P. U., Ahuja, A., Zylyftari, G., Lee. J. W., Morris, J. F. Rheology of cyclopentane hydrate slurry in a model oil-continuous emulsion. Rheologica Acta, 55, 235-243 (2016). https://doi.org/10.1007/s00397-016-0911-1

Kittel, C. Introduction to Solid State Physics, John Wiley & Sons, New York (2004).

Koga, K., Tanaka, H. Rearrangement dynamics of the hydrogen□bonded network of clathrate hydrates encaging polar guest. The Journal of Chemical Physics, 104, 263-273 (1996). https://doi.org/10.1063/1.470897

Kvenvolden, K. A. A review of the geochemistry of methane in natural gas hydrate. Organic Geochemistry, 23, 997-1008 (1995). https://doi.org/10.1016/0146-6380(96)00002-2

Lachance, J. W., Sloan, E. D., Koh, C. A. Effect of hydrate formation/dissociation on emulsion stability using DSC and visual techniques. Chemical Engineering Science, 63, 3942-3947 (2008). https://doi.org/10.1016/j.ces.2008.04.049

Larson, R. G. The Structure and Rheology of Complex Fluids, Oxford University Press, New York (1999).

Leopércio, B. C., Mendes, P. R. de S., Fuller, G. G. The Growth Kinetics and Mechanics of Hydrate Films by Interfacial Rheology. Langmuir, 32, 4203-4209 (2016). https://doi.org/10.1021/acs.langmuir.6b00703

Lingelem, M. N., Majeed, A. I., Stange, E. Industrial Experience in Evaluation of Hydrate Formation, Inhibition, and Dissociation in Pipeline Design and Operation. Annals of the New York Academy of Sciences, 715, 75-93 (1994). https://doi.org/10.1111/j.1749-6632.1994.tb38825.x

Menezes, D., Ralha, T. W., Franco, L. F. M., Pessôa Filho, P. de A., Fuentes, M. D. R. Simulation and Experimental Study of Methane-Propane Hydrate Dissociation by High Pressure Differential Scanning Calorimetry. Brazilian Journal of Chemical Engineering, 35, 403-414 (2018). https://doi.org/10.1590/0104-6632.20180352s20160329

Nakajima, M., Ohmura, R., Mori, Y. H. Clathrate Hydrate Formation from Cyclopentane-in-Water Emulsions. Industrial & Engineering Chemistry Research, 47, 8933-8939 (2008). https://doi.org/10.1021/ie800949k

Parent, J. S., Bishnoi P. R. Investigations into the nucleation behaviour of methane gas hydrates. Chemical Engineering Communications, 144, 51-64 (1995). https://doi.org/10.1080/00986449608936444

Parrish, W. R., Prausnitz, J. M. Dissociation Pressures of Gas Hydrates Formed by Gas Mixtures. Industrial & Engineering Chemistry Process Design and Development, 11, 26-35 (1972). https://doi.org/10.1021/i260041a006

Raman, A. K. Y., Koteeswaran, S., Venkataramani, D., Clark, P., Bhagwat, S., Aichele, C. P. A comparison of the rheological behavior of hydrate forming emulsions stabilized using either solid particles or a surfactant. Fuel, 179, 141-149 (2016a). https://doi.org/10.1016/j.fuel.2016.03.049

Raman, A. K. Y., Venkataramani, D., Bhagwat, S., Martin, T., Clark, P. E., Aichele, C. P. Emulsion stability of surfactant and solid stabilized water-in-oil emulsions after hydrate formation and dissociation. Colloids and Surface A: Physicochemical and Engineering Aspects, 506, 607-621 (2016). https://doi.org/10.1016/j.colsurfa.2016.06.042

Sakemoto, R., Sakamoto, H., Shiraiwa, K., Ohumura, R., Uchida, T., Clathrate Hydrate Crystal Growth at the Seawater/Hydrophobic-Guest-Liquid Interface. Crystal Growth & Design, 10, 1296-1300 (2010). https://doi.org/10.1021/cg901334z

Schick, M. J., Hubbard, A. T. Emulsions and Emulsion Stability, Taylor & Francis, London (2006).

Silva, P. H. de L., Naccache, M. F., Mendes, P. R. de S., Campos, F. B., Teixeira, A., Sum, A. K. Investigation into THF hydrate slurry flow behaviour and inhibition by an anti-agglomerant. Energy & Fuels, 31, 14385-14392 (2017). https://doi.org/10.1021/acs.energyfuels.7b02425

Shaw, D. J. Colloid & Surface Chemistry, Butterworth-Heinemann, London (1992).

Sloan, E. D., Gas Hydrates: Review of Physical/Chemical Properties. Energy & Fuels, 12, 191-196 (1998). https://doi.org/10.1021/ef970164+

Sloan, E. D. Introductory overview: Hydrate knowledge development. American Mineralogist, 89, 1155-1161 (2004). https://doi.org/10.2138/am-2004-8-901

Sun, D., Englezos, P. Determination of CO_2 Storage Density in a Partially Water-Saturated Lab Reservoir Containing CH_4 from Injection of Captured Flue Gas by Gas Hydrate Crystallization. The Canadian Journal of Chemical Engineering, 95, 69-76 (2017). https://doi.org/10.1002/cjce.22655

Tadros, T. F., Vincent, B. Emulsion stability, In. Encyclopedia of Emulsion Technology, ed. Becher, P., Dekker, M., New York, 129-285 (1983).

Vincent, S. Helping Ensure, Safe and Cost Efficient Oil Extraction For Our Energy Hungry World. Energy & Environment, 21, 461-467 (2010). https://doi.org/10.1260/0958-305X.21.5.461

Walstra, P. Principles of emulsion formation. Chemical Engineering Science, 48 333-349 (1993). https://doi.org/10.1016/0009-2509(93)80021-H

Yu, W., Xie, H. A Review on Nanofluids: Preparation, Stability Mechanisms, and Applications. Journal of Nanomaterials, 1-17 (2012). https://doi.org/10.1155/2012/435873

APPENDIX - Graphical TOC Entry